# A pharmacophore model for dopamine $D_4$ receptor antagonists

Jonas Boström[a], Klaus Gundertofte[b] & Tommy Liljefors[a,*]
[a]*Department of Medicinal Chemistry, Royal Danish School of Pharmacy, Universitetsparken 2, DK-2100 Copenhagen, Denmark;* [b]*H. Lundbeck A/S, Ottiliavej 9, DK-2500 Copenhagen-Valby, Denmark*

## Summary

A pharmacophore model for dopamine $D_4$ antagonists has been developed on the basis of a previously reported dopamine $D_2$ model. By using exhaustive conformational analyses (MM3* force field and the GB/SA hydration model) and least-squares molecular superimposition studies, a set of eighteen structurally diverse high affinity $D_4$ antagonists have successfully been accommodated in the $D_4$ pharmacophore model. Enantioselectivities may be rationalized by conformational energies required for the enantiomers to adopt their proposed bioactive conformations. The pharmacophore models for antagonists at the $D_4$ and $D_2$ receptor subtypes have been compared in order to get insight into molecular properties of importance for $D_2/D_4$ receptor selectivity. It is concluded that the bioactive conformations of antagonists at the two receptor subtypes are essentially identical. Receptor essential volumes previously identified for the $D_2$ receptor are shown to be present also in the $D_4$ receptor. In addition, a novel receptor essential volume in the $D_4$ receptor, not present in the $D_2$ receptor, has been identified. This feature may be exploited for the design of $D_4$ selective antagonists. However, it is concluded that the major determinant for $D_2/D_4$ selectivity is the nature of the interactions between the receptor and aromatic ring systems. The effects of the electronic properties of these ring systems on the affinities for the two receptor subtypes differ substantially.

## Introduction

Many of the symptoms of schizophrenia are considered to be caused by an excess of dopamine (DA) activity in the brain. The antipsychotic effects of neuroleptic drugs are presumed to be due to inhibition of DA receptors [1]. The classical neuroleptic drugs used in the treatment of schizophrenia generally induce major movement disorders, also known as extrapyramidal side effects, and it has been proposed that these side effects are due to blockade of DA $D_2$ receptors in the striatum [2]. Distribution studies indicate that the $D_4$ subtype of DA receptors is more abundant in the limbic and the cortical brain areas than in the striatum [3]. A highly favorable antipsychotic profile without extrapyramidal side effects is displayed by the atypical neuroleptic clozapine [4]. Clozapine has been reported to display higher affinity for the $D_4$ subtype of DA re-

ceptors than for the $D_2$ subtype [5]. Thus, selective $D_4$ receptor antagonists may have a potential as effective antipsychotics without the undesired extrapyramidal side effects displayed by the classical neuroleptics. Unfortunately, clozapine induces agranulocytosis in some patients and is therefore of limited therapeutical use. Therefore, recent years have seen a large activity in the development of new $D_4$ selective antagonists [6].

The DA receptors belong to the large superfamily of G-protein coupled receptors, which are all presumed to have a seven transmembrane helices structure. The dopamine receptors can be classified into $D_1$-like and $D_2$-like subfamilies. The $D_1$-like subfamily includes the $D_1$ and $D_5$ receptors while the $D_2$, $D_3$ and $D_4$ receptors belong to the $D_2$-like subfamily [6]. The $D_2$ and $D_4$ receptors display very high sequence identity [5] and it may therefore be expected

that ligands for these receptors have similar binding modes.

We have previously reported a pharmacophore model for DA $D_2$ receptor antagonists [7]. The development of this model was based on comprehensive conformational studies and subsequent molecular superimpositions of the two potent DA $D_2$ antagonists (S)-octoclothepin and (1R,3S)-tefludazine. The model has been thoroughly validated by studies on the enantiomers of octoclothepin [8], on phenylindanes, -indenes and -indoles [9], on a series of structurally different benzamides [10], and on thioxanthenes and butyrophenones [11]. Furthermore, the results of a study on the effect of aromatic substitution on the DA $D_2$ affinity of 1-piperazino-3-phenylindanes and 10-piperazino-10,11-dihydrodibenzo-[b,f]thiepins strongly support the model [12]. The $D_2$ pharmacophore model has been used in conjunction with a corresponding model for $5HT_{2A}$ receptor antagonists in a study on the molecular requirements for $5HT_{2A}/D_2$ selectivity [13].

Although a large number of selective DA $D_4$ antagonists have been published [6], no pharmacophore model for $D_4$ receptor antagonists has so far been reported in the literature. In the present work, we report the development of a pharmacophore model for antagonists at the DA $D_4$ receptor. The aim of this work is to compare the $D_4$ model with the corresponding model for DA $D_2$ receptor antagonists in order to gain insight into the molecular basis for $D_4/D_2$ receptor selectivity and ultimately to exploit this insight for the design of a new $D_4$ antagonist displaying selectivity with respect to the $D_2$ receptor. The compounds employed in the pharmacophore development are shown in Figure 1.

## Computational methods

### Force fields

Force field calculations were carried out using the MM3*, AMBER* and MMFF94S force fields implemented in MacroModel V6.5 [14]. As the torsional force constant C(sp2)-N(sp2)-O(sp2)-C(sp2) and the bond stretch constant N(sp2)-O(sp2) required for calculations on the isoxazole subunit in compound **16** are missing in MM3*, these parameters were taken from the MM3(94) force field parameter list [15]. All energy minimizations were carried out with the truncated Newton conjugate gradient algorithm (TNCG).

### Conformational analysis and identification of bioactive conformations

Conformational space was explored by using the Monte Carlo Multiple Minimum (MCMM) method implemented in the MacroModel program [16]. All heavy atoms and hydrogens on heteroatoms were superimposed in the test for duplicate structures. All rotatable single bonds were included in the conformational searches and these were terminated when the examination of the log file showed that each energy minimum structure had been found multiple times. The conformational searches were performed in aqueous solution using the GB/SA continuum model [17]. The N-protonated form of the molecules (see Figure 1), which is the prevalent species at physiological pH, was used in the calculations. The conformational energy penalty for binding, i.e. the conformational energy required for each of the ligands to adopt its proposed bioactive conformation, was calculated as the difference in internal energy between the bioactive conformation and the global energy minimum conformation obtained in aqueous solution. The internal energy for the global energy minimum conformation in aqueous phase is obtained by subtracting the hydration energy from the total energy. For a discussion of the necessity of using this procedure to calculate conformational energy penalties for receptor binding see Reference 18. As a guideline for acceptable conformational energy penalties, the value 3 kcal/mol as obtained by our previous calculations on ligand-protein complexes was employed. The bioactive conformation of each of the $D_4$ antagonists was deduced on the basis of a low conformational energy penalty and a low rms value (root mean squares deviation with respect to least-squares superimposition with the template molecule and the fitting points described below).

### Superimposition studies

The ammonium nitrogen, a site-point located 2.8 Å from the ammonium nitrogen in the nitrogen-hydrogen direction (simulating a hydrogen bond acceptor) and the centroids of the aromatic moieties as shown in Figure 1, were used as fitting points in the superimposition studies. Least-squares rigid body molecular superimpositions were performed by using the MacMimic program [19]. The quality of a superimposition was measured in terms of rms values of the fitting points. An rms value of 0.6 Å has been used as
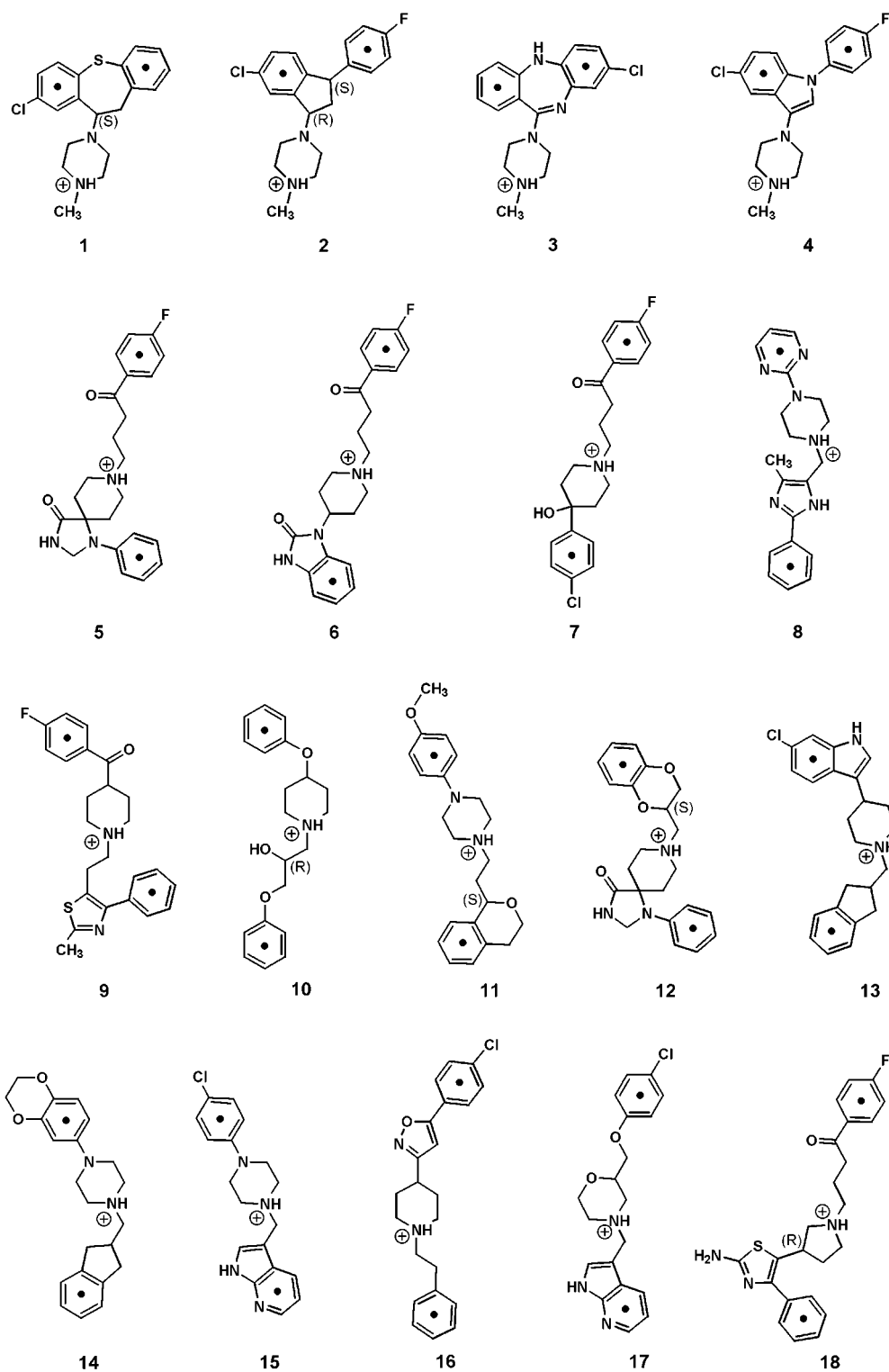
*Figure 1.* Structures of the ligands studied in this work. The centroids of the aromatic rings used as fitting points are indicated in the formulas. In those cases for which experimental data are available, the absolute configuration of the highest affinity enantiomer is given. The ligands are oriented according to their suggested binding mode.

a soft indicator to determine whether a fit is acceptable or not. Aromatic rings in the ligands were fitted in a coplanar orientation with respect to the aromatic pharmacophore elements. It should be mentioned that the rms values do not give any measure of this coplanarity. The template fitting procedure implemented in the Flo96 program [20] was used in some cases discussed below. This procedure allows a simultaneous minimization of the internal energy of the molecules to be fitted and an optimization of the fit in terms of minimization of superimposition energy.

*Quantum chemical calculations*

*Ab initio* calculations (HF/6-31G*) on the conformational energy difference between the planar and the orthogonal conformations of the pyrimidyl-piperazine subunit in compound **8** were performed by using Gaussian98 [21].

The semi-empirical methods AM1-SM5.4A and PM3-SM5.4P implemented in the AMSOL program [22] were used for calculations of conformational energies and free energies of hydration for compounds **5**–**7**, **9**–**12** and **21**. The calculations were performed for the N-protonated species and the solvation energy was calculated as the energy difference between the optimized structures in aqueous phase and in the gas phase.

## Results and discussion

### The DA $D_2$ pharmacophore model

As mentioned in the Introduction, our previously reported DA $D_2$ pharmacophore model is based on comprehensive conformational analyses and superimposition studies of the two high-affinity $D_2$ receptor antagonists (S)-octoclothepin (**1**) and (1R,3S)-tefludazine (Figure 2) [7]. A superimposition of the proposed bioactive conformations of these compounds is shown in Figure 2a and the relative orientations in space of the pharmacophore elements (fitting points) **A**-**D** derived from the superimposition are displayed in Figure 2b. The basic $D_2$ pharmacophore model was extended by Andersen et al. in connection with studies on the effect on the $D_2$/5HT$_{2A}$ selectivity of aromatic substitutions in indole analogues of **2** [13]. This study made it possible to define two important receptor essential volumes, **E** and **F** in Figure 2b, in the $D_2$ pharmacophore model. These volumes indicate positions in space in which the presence of molecular

fragments or substituents lead to a significantly decreased DA $D_2$ affinity. The arrow in Figure 2b points at the so-called 'neuroleptic position'. A substituent in this position in general increases the DA $D_2$ affinity of the ligand.

### The basis for the development of the DA $D_4$ pharmacophore model

The uniqueness of the $D_2$ pharmacophore model with respect to the relative orientations of the piperazine rings and the tricyclic ring systems in (S)-**1** and (1R,3S)-tefludazine was considerably strengthened by a study on the enantiomers of **1** [8]. The enantioselectivity of these enantiomers with respect to the $D_2$ receptor is low. As shown in Table 1, the (S)-**1** enantiomer displays only 2.5 times higher affinity for the $D_2$ receptor than (R)-**1**. The conformational flexibility of **1** makes it possible for (S)-**1** and (R)-**1** to adopt very similar 3D-shapes (see inserted superimposition of the proposed bioactive conformations in Figure 3). An analysis of the calculated potential energy curves for rotation about the bond connecting the piperazine ring and the tricyclic ring system in (S)-**1** and (R)-**1** in their superimposed conformations (Figure 3) showed that there exists only one mutual low energy region. The arrow in Figure 3 points at the dihedral angle value of the proposed bioactive conformation of (S)-**1**, as obtained by the superimposition study of (S)-**1** and (1R,3S)-tefludazine discussed above (Figure 2a), and the corresponding value for (R)-**1** in the superimposition shown in Figure 3. The calculated conformational energy difference between the proposed bioactive conformations of the enantiomers of **1** was found to be in good agreement with the observed relative affinities of the enantiomers [8]. It should be noted that in the previous study on the enantiomers of **1**, the potential energy curves were calculated for the non-protonated compounds in the gas phase. However, as we have recently shown, the appropriate quantities to be used in the calculations of conformational energy penalties for binding of ligands to enzymes and receptors is the internal energy difference between the bioactive conformation and the global energy minimum in aqueous solution [18]. Thus, in the context of the present work the potential energy curves displayed in Figure 6 in Reference 8 have been recalculated for N-protonated (S)-**1** and (R)-**1** in aqueous solution by using the MM3* force-field and the GB/SA hydration model (see Computational Methods section). As the results shown in Figure 3 are virtually identical to
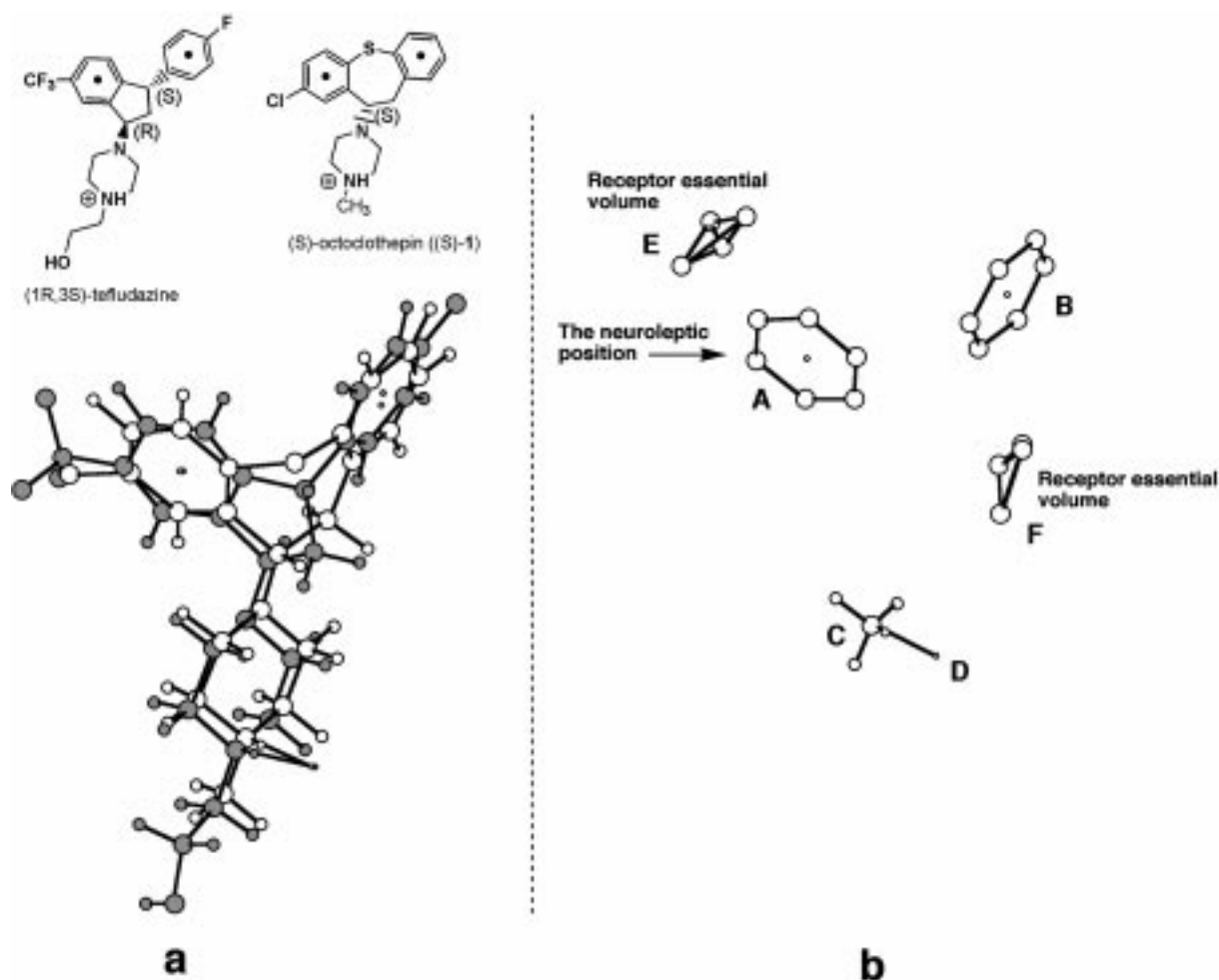
*Figure 2.* (a) Least-squares superimposition of (S)-octoclothepin and (1R,3S)-tefludazine. (b) The basic $D_2$ pharmacophore model based on this superimposition. The model includes four pharmacophore elements, two elements (**A** and **B**) corresponding to the aromatic rings, an ammonium nitrogen (**C**) and a site point in the $N^+$-H direction (**D**). In addition, the model includes two receptor essential regions (**E** and **F**).

those obtained in the previous work (cf. Figure 6 in Reference 8), the conclusions based on the previous calculations are all valid.

In view of the usefulness of employing the enantiomers of **1** in the development and validation of the $D_2$ model, the DA $D_4$ receptor affinities of (S)-**1** and (R)-**1** were determined in order to find out if a similar analysis could be employed in the $D_4$ case. As shown in Table 1, both enantiomers of **1** are found to be high-affinity DA $D_4$ antagonists, the (S)-**1** enantiomer displaying a higher affinity than (R)-**1** by only a factor of 3. Thus, the relative DA $D_4$ affinities of (S)-**1** and (R)-**1** are virtually identical to that displayed by the enantiomers at the DA $D_2$ receptor (Table 1). According to our previous analysis [8], this strongly indicates that the bioactive conformations of the enantiomers

of **1** are essentially identical to that displayed by those compounds at the DA $D_2$ receptor. This implies that the basic DA $D_2$ pharmacophore model including pharmacophore elements **A**-**D** in the relative positions displayed in Figure 2b may be used as a starting point for the development of a pharmacophore model for antagonists at the $D_4$ receptor and that (S)-**1** may be used as a template compound. This observation implies that $D_2/D_4$ selectivity cannot be rationalized in terms of differences in bioactive conformations at the two receptor subtypes with respect to those parts of the molecules described by pharmacophore elements **A–D**.

*Table 1.* Calculated (MM3*) conformational energy penalties ($\Delta E_{conf}$), rms values from least-squares superimposition to the pharmacophore model and $D_4$ and $D_2$ receptor affinities for ligands **1–18**

| Compound | $\Delta E_{conf}$ (kcal/mol) | Rms value (Å) | Receptor affinities | | Ref. |
|---|---|---|---|---|---|
| | | | $D_4/K_i$ (nM) | $D_2/K_i$ (nM) | |
| (S)-**1** | 1.2 | 0.00 | 1.5 | 2.8[a] | 23 |
| (R)-**1** | 1.9 | 0.40 | 4.5 | 7.1[a] | 23 |
| **2** | 0.9 | 0.25 | 15 | 4.6 | 23 |
| **3** | 2.6 | 0.34 | 31 | 37 | 23 |
| **4** | 0.5 | 0.54 | 6.5 | 1.3 | 23 |
| **5** | 0.0 | 0.13 | 0.2 | 0.2 | 23 |
| **6** | 2.2 | 0.27 | 1.9 | 0.4 | 23 |
| **7** | 2.1 | 0.42 | 2.9 | 0.9 | 23 |
| **8** | 0.6[b] | 0.61 | 6.0 | 1440 | 24 |
| **9** | 6.6 | 0.35 | 2.1 | 226 | 25 |
| **10** | 6.0 | 0.48 | 2.0 | 244 | 26 |
| **11** | 4.6 | 0.71 | 2.2 | 792 | 27 |
| **12** | 7.2 | 0.49 | 8.7[c] | 0.2 | 37 |
| **13** | 0.5 | 0.32 | 1.9 | 51.4 | 23 |
| **14** | 0.9 | 0.68 | 1.6 | 800 | 28 |
| **15** | 0.7 | 0.78 | 0.43 | 960 | 29 |
| **16** | 1.8 | 0.54 | 3.5 | >1700 | 30 |
| **17** | 2.4 | 0.78 | 1.5 | >1700 | 31 |
| **18** | 2.4 | 0.72 | 5.2 | 545 | 32 |

[a] These values differ slightly from those previously reported [8]. The new data have been measured by using a DMSO solution of the compound rather than a water solution.
[b] This value differs from that in Figure 6, where the corresponding value calculated by MMFF94S is given.
[c] Binding affinity for the racemate [23].

## Conformational analysis and superimposition studies of DA $D_4$ receptor antagonists

The calculated conformational energy penalties of the proposed bioactive conformations for compounds **1–18** obtained as described in the Computational Methods section and the rms values obtained by the least-squares fitting to the pharmacophore model in Figure 1b and its extensions as described below are given in Table 1. This table also includes the observed DA $D_4$ and $D_2$ receptor affinities. The data in Table 1 will be discussed below for the different structural classes of compounds and the proposed binding modes of these compounds.

### Receptor antagonists **1–4**

Many of the classical $D_2$ receptor antagonists incorporate a tricyclic ring system. Compounds **1–4**, which also display high affinities for the $D_4$ receptor (Table 1), have been chosen to represent this family of compounds. Figure 4 displays the results of a least-squares fitting of the tricyclic compounds (R)-**1**, (S)-**1**, (1R,3S)-**2** [9], **3** and **4** [33] to pharmacophore elements **A-D** in Figure 2b. The calculated conformational energies and rms values are all low for the proposed bioactive conformations of **1–4** (Table 1).

As mentioned above, a study on the effects of substituents in the tricyclic ring system on the $D_2$ and $5HT_{2A}$ receptor affinities led to the identification of the receptor essential regions **E** and **F** in the $D_2$ pharmacophore model (Figure 2b). In order to investigate if these receptor essential regions also are present in the $D_4$ receptor, compounds **2**,**19a-b** and **20a-d** were studied. The data shown in Table 2 display virtually identical effects on the $D_2$ and $D_4$ receptor affinities of the introduction of a methyl substituent in the positions shown in the table. The reduced $D_2$ and $D_4$ affinities of **19b** compared to **19a** and of **20d** compared to **20a** show that a methyl group in the $R_3$ position occupies a receptor essential region (**E** in Figure 2b) in
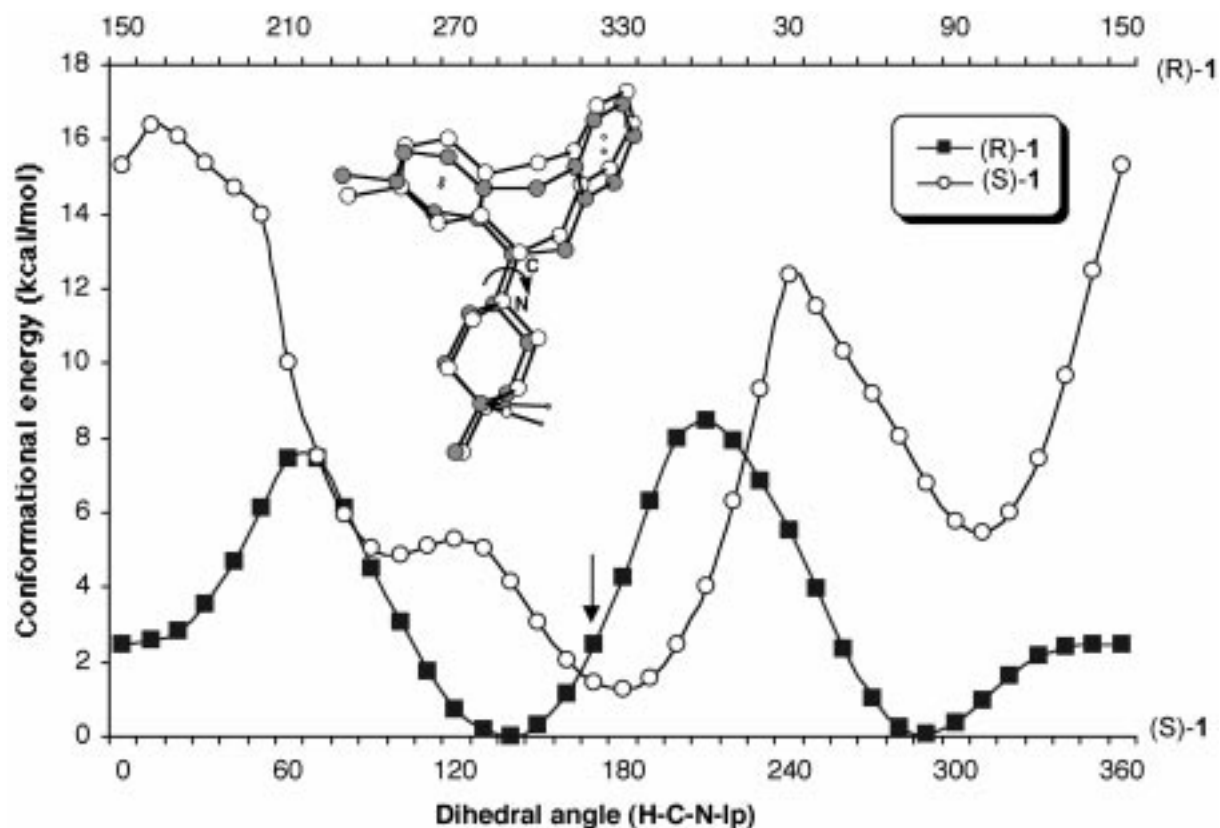
*Figure 3.* Calculated potential energy curves (MM3\*-GB/SA) for rotation about inter-ring C-N bond in (S)-**1** and (R)-**1**. The arrow points at the dihedral angle values corresponding to the proposed bioactive conformations.

both receptor subtypes. The strongly reduced affinity of **20b** compared to **20a** shows that a methyl in the $R_1$ position also occupies a disallowed region (**F** in Figure 2b) in both receptor subtypes. In conclusion, all pharmacophore elements in the $D_2$ pharmacophore model shown in Figure 2b including the receptor essential volumes **E** and **F** are also present in the $D_4$ pharmacophore model. In addition, the data in Table 2 shows that a methyl and a chloro substituent in the $R_2$ position (the 'neuroleptic position' in Figure 2b) increases the affinity for both receptor subtypes. Thus, in contrast to the case of $5HT_{2A}$ vs $D_2$ receptors discussed above, $D_4$-selectivity with respect to the $D_2$ receptor cannot be achieved by substitutions in positions corresponding to $R_1,R_2$ and $R_3$ in **19a** and **20a**.

*Extension of the pharmacophore model*

The butyrophenones (**5–7**) are nontricyclic DA $D_2$ and $D_4$ antagonists that incorporate N-alkyl substituents that are essential for receptor binding. Previously,

spiperone (**5**) has been accommodated in the $D_2$ model [11]. As shown in Figure 5, compound **5** may be straightforwardly fitted in its global energy minimum conformation to the pharmacophore elements **B**, **C** and **D** in Figure 2b.

The $D_2$ and $D_4$ receptor affinities of compound **21** are 57 and 740 nM, respectively [23]. Thus, the very high $D_4$ as well as $D_2$ affinities of compounds **5–7** (Table 1) are most likely due to strong attractive interactions between the receptors and the 1-phenyl-1,3,8-triazaspiro-[4.5]decan-4-one moiety in **5**, the 1,3-dihydro-benzoimidazol-2-one system in **6** [34], and the phenyl ring and hydroxy substituent on the piperidine moiety in **7**. These substituents dramatically increase the $D_2$ and $D_4$ affinities of **5–7** in comparison to the 4-methyl substituent in **21**. In order to make sure that these affinity increases are not due to favorable differences in solvation energies for **5–7** in comparison to **21**, the free energies of hydration for these compounds were calculated by using the AM1-SM5.4A method (see Computational Methods

*Table 2.* Receptor affinities for compounds **2**, **19a**–**b** and **20a-d** [23]



| Compound | Structure | Substituent | Receptor affinities | |
|---|---|---|---|---|
| | | | $D_4/K_i$ (nM) | $D_2/K_i$ (nM) |
| **19a** | I | $R_2, R_3 = H$ | 80 | 43 |
| **2** | I | $R_2 = Cl$ | 15 | 4.6 |
| **19b** | I | $R_3 = Cl$ | 150 | 160 |
| **20a** | II | $R_1, R_2, R_3 = H$ | 60 | 8.9 |
| **20b** | II | $R_1 = Me$ | 1050 | 157 |
| **20c** | II | $R_2 = Me$ | 26 | 5.4 |
| **20d** | II | $R_3 = Me$ | 240 | 80 |

section). The free energies of hydration for **5**–**7** are calculated to be more negative than that for **21** by 3.5, 9.5 and 4.5 kcal/mol, respectively. Thus, the desolvation energies of **5**–**7** are significantly larger than that of **21**, supporting the conclusion that there exist strong specific interactions between the piperidyl substituents in **5**–**7** and both receptor subtypes.

By using the template fitting procedure in the Flo96 program (see Computational Methods section), including a simultaneous minimization of the internal energy of the molecule and optimization of the fit produced a very good superimposition of the aromatic rings in **5**–**7** (Figure 5). The common position of the aromatic rings in **5**–**7** defines a new pharmacophore element **G** (Figure 5) for the D$_4$ as well as for the D$_2$ pharmacophore model. This pharmacophore element will be used for the fittings of compounds **8**–**18** to the model as discussed below.

*The fitting of compound **8** to the pharmacophore model*

The great majority of the dopamine D$_4$ selective antagonists studied in the present work (Figure 1) do not belong to the class of tricyclic compounds exemplified by **1**–**4** and they generally incorporate aromatic moieties at both ends of the molecule. Thus, many of the D$_4$ antagonists studied in this work seem to be able to be superimposed on the model displayed in Figure 5 in two or more different modes. It is therefore important to determine how such ligands should be oriented in the model with respect to the pharmacophore elements **A**, **B** and **G** (Figure 5). The D$_4$ selective antagonist **8** is a typical example illustrating this problem and the procedures used to solve the problem. As displayed in Figure 6, there are in this particular case three different reasonable orientational possibilities to fit compound **8** to the pharmacophore elements of the model. Compound **8** has a pyrimidine ring attached

*Figure 4*. Least-squares superimposition of (R)-**1**, (S)-**1**, (1R,3S)-**2**, **3** and **4**. Hydrogens are removed for clarity.

to the piperazine ring. The conformational energy for rotation about the bond connecting these rings may be of importance for the conformational energy penalties for possible bioactive conformations of **8**. In order to assess the ability of the MM3* force field to calculate these conformational energies, *ab initio* calculations (HF/6-31G*) were performed for the conformational energy difference between the 'coplanar' (N(sp2)-C-N(sp3)-lonepair = 90 deg) and the 'orthogonal' (N(sp2)-C-N(sp3)-lonepair = 0 deg) conformations of the pyrimidyl-piperazine subunit. The calculations show a large energy difference between the 'coplanar' and the 'orthogonal' forms, 9.7 kcal/mol favoring the 'coplanar' form. The MM3* force field fails to reproduce this large energy difference giving an energy difference of only 1.6 kcal/mol. However, the calculated energy difference obtained by using the MMFF94S force field is 8.5 kcal/mol, in good agreement with the HF/6-31G* result. Since it is important for this case to be able to accurately calculate the conformational energies involving the pyrimidyl-piperazine subunit, the MMFF94S force field was employed to calculate the conformational energies for the three alternative binding modes of compound **8** shown in Figure 6. In binding mode **I**, the pharmacophore elements **A**, **C**, **D** and **G** are used for fitting. The same pharmacophore elements are employed in mode **II**, but the molecule

is fitted upside-down compared to mode **I**. In binding mode **III**, pharmacophore elements **B**,**C**, **D** and **G** are being used.

On comparing the conformational energies required for **8** to adopt the three different binding modes, it is clear that mode **I** is the only acceptable alternative. The relatively high rms value in this superimposition will be discussed below. Modes **II** and **III** may be ruled out on the basis of prohibitively high conformational energies, 14.1 kcal/mol and 19.3 kcal/mol, respectively. Approximately 10 kcal/mol of the conformational energy penalty comes from the high-energy 'orthogonal' form of the pyrimidinyl-piperazine unit used to obtain an optimal fit to the model. Furthermore, binding modes **II** and **III** are incompatible with the pharmacophore model due to conflicts with receptor essential volumes or the N-H interaction site. The arrows in Figure 6 denote destructive ligand-receptor interactions caused by the methyl substituent in **8**. In mode **II**, the methyl group is partly overlapping the receptor essential volume **F**. In mode **III**, the five-membered heterocyclic ring is very close to this receptor essential volume and, more important, the methyl group is located close to the site point **D** which should cause steric repulsive interactions with this interaction site. Thus, on the basis of this analysis it is concluded that binding mode **I** is the only one compatible with the pharmacophore model.

*Antagonists **8**–**15** fitted to the pharmacophore elements **A**, **C**, **D** and **G***

Compounds **8**–**15** may be fitted to the model by using the pharmacophore elements **A**, **C**, **D** and **G**. A superimposition of the calculated bioactive conformations is displayed in Figure 7. The corresponding calculated conformational energy penalties for the bioactive conformations and the rms values are given in Table 1. The higher than average rms values for **8** as well as for the phenyl-piperazines **11**, **14** and **15** is a consequence of the representation of the aromatic ring by its centroid. If a close fit of such centroids to the model is required this implies a very strong and in some cases most probably unrealistic requirement of the degree of fit of an aromatic ring to its binding site in the receptor. The average distance between the centroid in pharmacophore element **A** and the aromatic centroid in the ligands **8**, **11**, **14** and **15** is twice as large as the corresponding distance for **9**, **10**, **12** and **13** [35] which do not contain a phenyl-piperazine moiety.
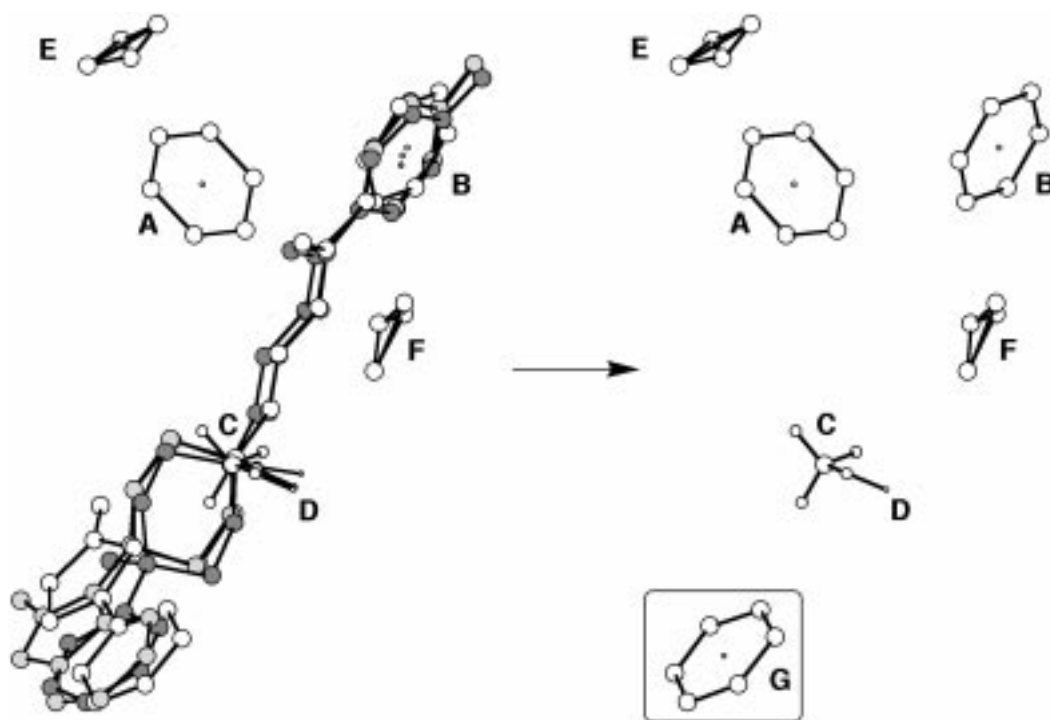
*Figure 5.* Compounds **5** (dark grey), **6** (light grey) and **7** (unfilled atoms) fitted to pharmacophore elements **A-D** of the $D_2/D_4$ pharmacophore model. The new pharmacophore element **G** is displayed in the model to the right.

Considering their high $D_4$ receptor affinities, compounds **9**–**12** display unexpectedly high conformational energy penalties, 4.6–7.2 kcal/mol (Table 1). The proposed bioactive conformations of **9**–**12** are shown in Figure 8a and the calculated lowest energy conformations of these compounds in aqueous phase (MM3*-GB/SA) are shown in Figure 8b. As shown in Figure 8b, compounds **10**–**12** all display internal hydrogen bonds in their global energy minima. These hydrogen bonds are broken in their proposed bioactive conformations (Figure 8a) resulting in a strong increase in internal energy. Compound **9** displays a combined hydrophobic/electrostatic 'collapse' (attractive vdW interactions and a cation-$\pi$ interaction) in the global aqueous phase minimum that is not present in the proposed bioactive conformation.

We have previously shown that the MM3*-GB/SA methodology may not be adequate for reliable calculations on the conformational properties for strongly polar molecules [18]. To determine if the 'collapses' displayed in Figure 8b are force field dependent and/or due to an insufficient dielectric continuum model, the corresponding results obtained by using the AMBER* and MMFF force fields in combination with the GB/SA hydration model and by using the semi-empirical quantum chemistry method PM3 in combination with the SM5.4P hydration model were investigated. The calculated energy differences (extended-'collapsed' conformation) are given in Table 3. While all three force fields calculate the 'collapsed' conformations shown in Figure 8b to be the most stable ones ($\Delta E_{tot} > 0$), the PM3-SM5.4P method predicts the extended structure (Figure 8a) of **9**, **11** and **12** to be of lowest energy. It is not clear which of the predictions are correct, but the high conformational penalties calculated for the high affinity compounds **9**, **11** and **12** indicate that force-field methods predict the 'wrong' conformation as the global energy minimum conformation in aqueous solution for these compounds. The internal conformational energy differences ($\Delta E_{conf}$) for **9**, **10** and **12** as calculated by the PM3-SM5.4P method (in Table 3) are clearly compatible with their high DA $D_4$ receptor affinities. However, the conformational energy difference for **11** calculated with the semi-empirical method, 5.2 kcal/mol (Table 3), is still somewhat higher than expected for a high affinity compound.
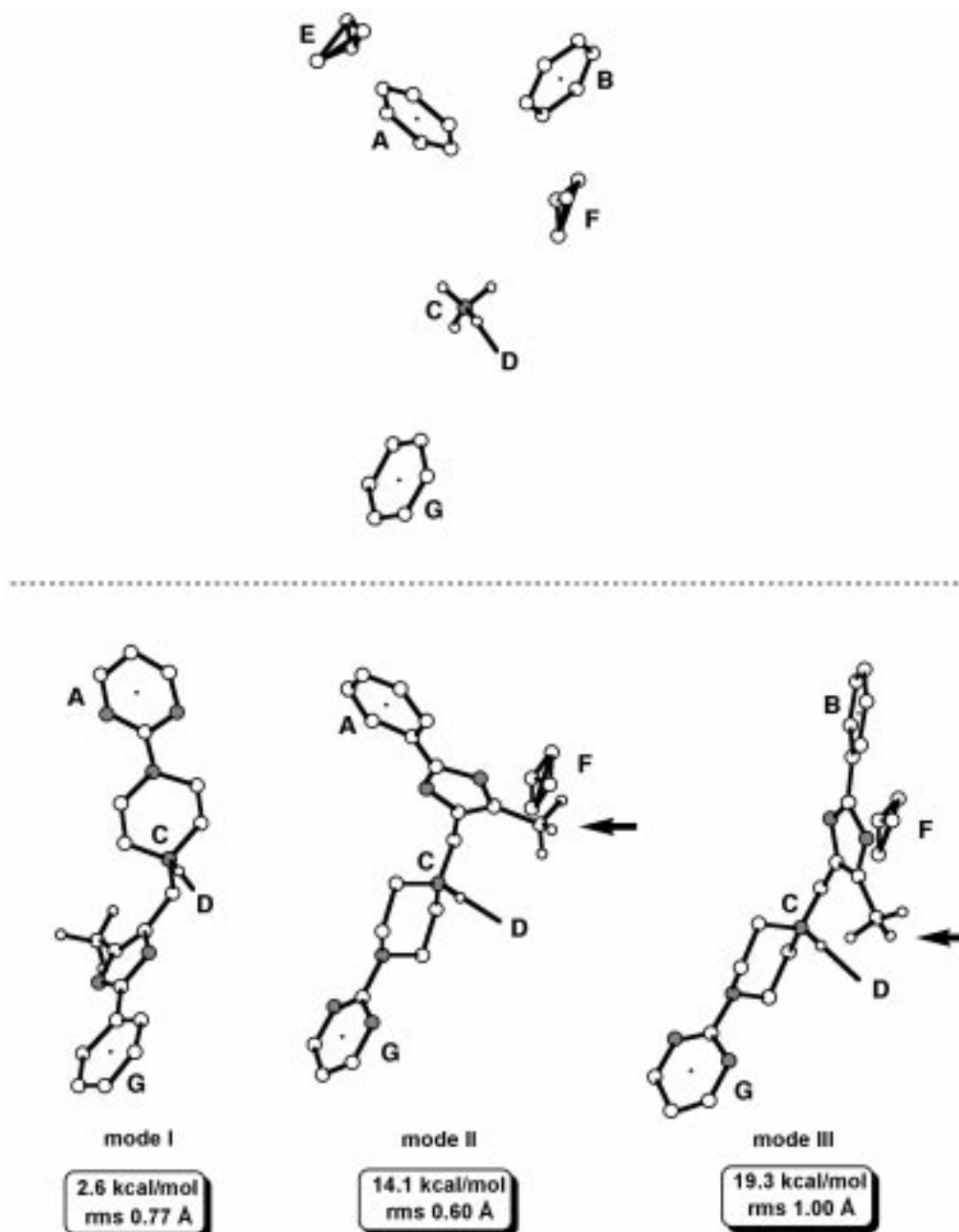
*Figure 6.* Three alternatives for fitting the D$_4$ selective antagonist **8** to the pharmacophore model. The arrows denote destructive ligand-receptor interactions. Calculated conformational energies (MMFF94S) and rms values are given below the different conformations.

### Antagonists **16**–**18** *fitted to the pharmacophore elements* **B**, **C**, **D** *and* **G**

No acceptable fits of compounds **16**–**18** to the pharmacophore model by employing pharmacophore element **A** could be obtained. However, these compounds could nicely be fitted to the model using the phar-macophore elements **B**, **C**, **D** and **G** with low con-formational energies (Table 1). A superimposition of the proposed bioactive conformations of these com-pounds and compounds **5**–**7** is displayed in Figure 9. Compounds **5**–**7** have been discussed above. Thus, it is proposed that the nonselective DA D$_4$ and D$_2$ re-ceptor antagonists **5**–**7** and the highly selective DA D$_4$

*Figure 7.* Compounds **8–15** fitted to the pharmacophore model with respect to pharmacophore elements **A**, **C**, **D** and **G**. Hydrogens are removed for clarity.

antagonists **16–18** display a different bonding mode than the antagonists **8–15**. The relatively high rms values of **17** and **18** are due to nonoptimal fitting of the N-alkyl substituents to the pharmacophore element **G** (Figure 5). For instance, the distance between the ammonium nitrogen and the centroid of the pyridine ring in **17** is shorter (by 1.3 Å) than the corresponding distance between pharmacophore elements **C** and **G**. However, as high affinity DA $D_4$ antagonists with N-benzyl substituents have been reported [6b, 30, 36], it is highly probable that the receptor site interacting with the N-alkyl substituents has a greater extension in space than described by the pharmacophore element **G**.

*Enantioselectivity*

For flexible chiral compounds it may be possible to superimpose one conformation of one enantiomer with another conformation of the other enantiomer. If such conformations fulfill the requirements of a pharmacophore model, the enantioselectivity of the com-

pounds may be rationalized or predicted on the basis of the difference in the conformational energies required for the enantiomers to adopt the bioactive conformation [8]. This provides a good test of a pharmacophore model. An example of this, the enantioselectivity of **1**, has been discussed above. The difference in calculated conformational energies of (S)-**1** and (R)-**1** closely corresponds to the difference in their free energies of binding [8]. In addition to **1**, there are six other chiral compounds, **2**, **10–12**, **17** and **18**, in the set of $D_4$ antagonists shown in Figure 1. Receptor binding data are available for the enantiomers of all of these compounds except **17** (unfortunately only $D_2$ data are available for compound **12**). The enantiomers of **2** cannot adopt superimposable conformations. In compound **10**, the hydroxy group at the chiral center may be involved in different receptor interactions in the enantiomers which makes this compound less suitable for calculations of enantioselectivity in terms of conformational energy differences. However, both enantiomers of each of the compounds **11**, **12** and **18** may adopt superimposable conformations that are compatible with the pharmacophore model. Least-squares superimpositions of the enantiomers of **11**, **12** and **18** in their deduced bioactive conformations are shown in Figure 10 and the calculated conformational energy penalties, the rms values of the fits and the receptor binding data ΔG are given in Table 4.

The enantiomers of **11** may be fitted to the $D_4$ and $D_2$ models with virtually identical rms values (Table 4). The (S)-enantiomer has a higher affinity to the $D_4$ and $D_2$ receptor than the (R)-enantiomer by a factor of 11 and >2, respectively. The calculated conformational energy penalty for the bioactive conformation of the (R)-enantiomer is 3.6 kcal/mol higher than that for the (S)-enantiomer. Thus, the calculations predict the (S)-enantiomer to be the most active one in agreement with experiments but the degree of enantioselectivity is somewhat overestimated. This may be due to differences in receptor interactions with the non-overlapping saturated heterocyclic rings (see Figure 10).

The enantiomers of **12** both display a very good fit to the pharmacophore model (Figure 10, Table 4). The calculated bioactive conformations are very similar and this is a particularly well-suited case for the prediction of enantioselectivity from calculated conformational energy penalties. Both enantiomers have significant $D_2$ receptor affinities (Table 4), the (S)-enantiomer displaying 7 times higher affinity than the (R)-enantiomer corresponding to a free energy dif-
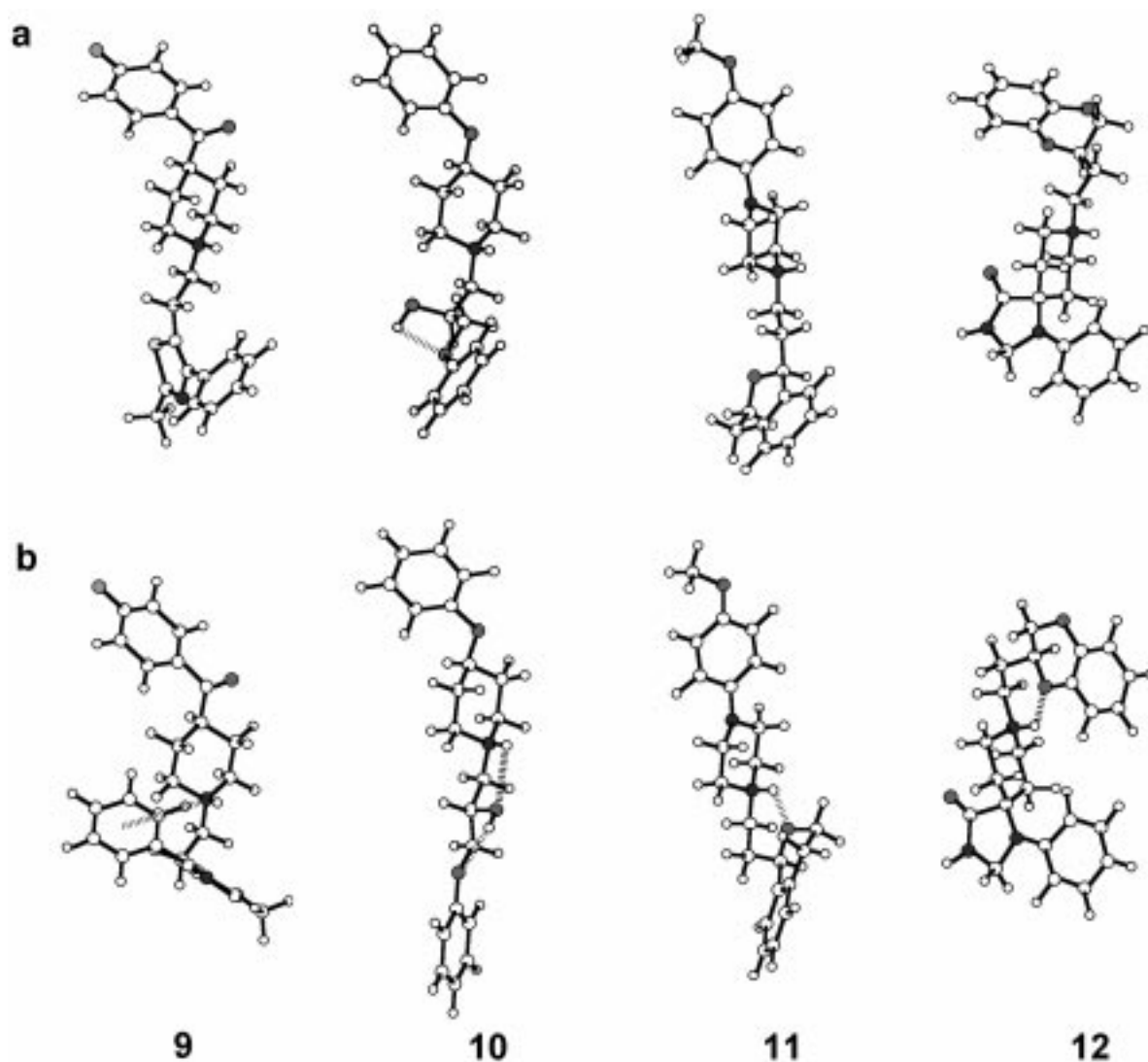
*Figure 8.* (a) The proposed bioactive conformations and (b) the calculated (MM3*-GB/SA) lowest energy conformations for compounds **9**–**12**.

*Table 3.* The total energy including solvation ($\Delta E_{tot}$) and conformational energy penalties ($\Delta E_{conf}$) for **9**–**12** using four different computational methods[a]. The energies are given in kcal/mol

| Method | **9** | | **10** | | **11** | | **12** | |
|---|---|---|---|---|---|---|---|---|
| | $\Delta E_{tot}$ | $\Delta E_{conf}$ | $\Delta E_{tot}$ | $\Delta E_{conf}$ | $\Delta E_{tot}$ | $\Delta E_{conf}$ | $\Delta E_{tot}$ | $\Delta E_{conf}$ |
| MM3* – GB/SA | 0.4 | 5.9 | 3.8 | 5.8 | 0.3 | 54.8 | 4.0 | 8.2 |
| AMBER* – GB/SA | 0.3 | 4.4 | 5.4 | 11.8 | 3.5 | 13.4 | 5.5 | 9.6 |
| MMFF – GB/SA | 2.2 | 8.0 | 5.3 | 10.5 | 0.3 | 57.8 | 4.6 | 7.5 |
| PM3 – SM5.4P | −2.5 | 0.1 | 2.0 | 51.7 | −1.0 | 55.2 | −0.7 | 3.5 |

[a] The proposed bioactive conformation and the global energy minimum in aqueous phase calculated by MM3* were used as input structures for the energy minimizations. $\Delta E_{tot}$ is the total energy difference between the extended and 'collapsed' conformations including solvation energy and $\Delta E_{conf}$ the difference in internal energies (solvation energies excluded).

*Table 4.* Calculated relative conformational energy penalties ($\Delta\Delta E_{conf}$), rms values and receptor binding data[a] for the enantiomers of **11** [27], **12** [37] and **18** [32]

| Compound | $\Delta\Delta E_{conf}$ (kcal/mol) | Rms value (Å) | Receptor affinities | |
|---|---|---|---|---|
| | | | $D_4/K_i$ (nM) | $D_2/K_i$ (nM) |
| (S)-**11**[b] | 0.0 | 0.71 | 2.2 (2.0–2.5) | 790 (590–1100) |
| (R)-**11**[b] | 3.6 | 0.69 | 24 (23–28) | >1800 |
| (S)-**12**[c] | 0.0 | 0.49 | N.A.[f] | 0.22 ± 0.02 |
| (R)-**12**[d] | 1.8 | 0.55 | N.A.[f] | 1.45 ± 0.06 |
| (S)-**18**[e] | 2.7 | 0.42 | 121[g] | 423[g] |
| (R)-**18**[e] | 0.0 | 0.72 | 5.2[g] | 545[g] |

[a]The numbers in parentheses represent 95% confidence intervals associated with the $K_i$ values.
[b]Optical purity estimated to be >99.5% ee [27].
[c]Optical purity found to be 95.3% ee [37].
[d]Optical purity found to be 94.2% ee [37].
[e]Optical purity not available.
[f]Binding data not available.
[g]Binding data given as $IC_{50}$ values.

ference of 1.1 kcal/mol. The conformational energy penalty of the bioactive conformation of the more potent (S)-enantiomer is calculated to be 1.8 kcal/mol lower in energy than the corresponding energy of the (R)-enantiomer, in good agreement with the observed difference in free energy of binding. Unfortunately, the $D_4$ receptor affinities for (S)-**12** and (R)-**12** are not available. However, since the enantiomers of compound **12** are fitted to pharmacophore elements which, according to the discussion above, are proposed to be virtually identical for the $D_2$ and $D_4$ receptors, the calculations predict that the (S)-enantiomer should be the highest affinity one also at the $D_4$ receptor.

(R)-**18** displays 23 times higher binding affinity for the $D_4$ receptor than (S)-**18** (Table 4) corresponding to a difference in free energy of binding of 1.9 kcal/mol. The calculated conformational energy penalty is 2.7 kcal/mol lower for the (R)-enantiomer than for the (S)-enantiomer, in agreement with the higher affinity of the (R)-enantiomer. Furthermore, the calculated difference in free energies of binding is in good agreement with the observed energy difference. Interestingly, the enantiomers of **18** are reported to have very similar affinities for the $D_2$ receptors (Table 4). As the phenyl-thiazol parts of the enantiomers of **18** do not superimpose optimally (Figure 10), and as the fit to the pharmacophore model is significantly better for the (S)-enantiomer (Table 4), it may be speculated that the requirement on the position of this part of the molecule is more strict for the $D_2$ than for the $D_4$ receptor. Thus, the better fit of (S)-**18** may at the

$D_2$ receptor compensate for the higher conformational energy penalty.

*Selectivity for the DA $D_4$ receptor*

The most important information provided by a pharmacophore model is the bioactive conformation of each ligand and the alignment of these conformations. A correct molecular alignment makes it possible to identify the structural relationships between different types of ligands. In addition, a correct molecular alignment may reveal receptor-essential volumes or other common features that may not be obvious from visual inspection of individual ligands. The results discussed above for the affinity to the $D_4$ receptor vs the $D_2$ receptor show that $D_2/D_4$ selectivity is not due to conformational differences of the bioactive conformations at the two receptors. Furthermore, the receptor essential volumes previously identified for the $D_2$ receptor are also present in the $D_4$ receptor, excluding the possibility to exploit such differences in the design of selective compounds. This is in contrast to our studies on $D_2/5HT_{2A}$ selectivity discussed above in which it also was concluded that the bioactive conformations are virtually the same at the two receptors but differences in receptor essential volumes could be identified and exploited.

Scanning the literature for differential substituent effects for ligands at the $D_4$ and $D_2$ receptor, one possible difference in receptor essential volumes for the two receptors was found. TenBrink et al. [27] have shown that a replacement of the methoxy group in **11**
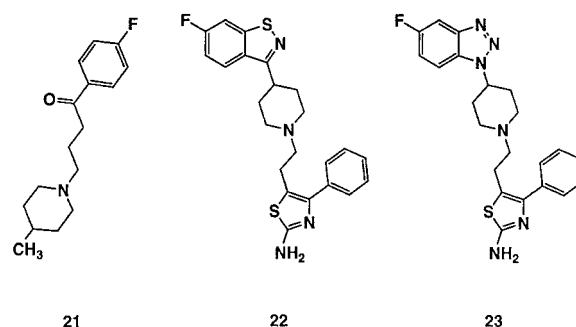
creases the $D_2$ affinity whereas the $D_4$ affinity remains largely unaffected. These results indicate a possibility to obtain or increase $D_2/D_4$ selectivity by using large substituents in the appropriate position.

The substantial selectivities observed for, for instance, compounds **8–11**, **13–18** (Table 1) cannot be rationalized within the framework of the pharmacophore models. In all cases the compounds display a good fit to the $D_4$ as well as to the $D_2$ pharmacophore models. Analyzing the structural characteristics of compounds **1–18** against the background of these results, we conclude that the major source of $D_2/D_4$ selectivity is to be found in the *properties* of the receptor sites interacting with pharmacophore elements **A**, **B** and **G** in the two receptors. The arguments for this are as follows.

The $D_2/D_4$ selectivity for the desmethyl analog of **8** increases from 49 to 592 by replacing the pyrimidinyl ring by a phenyl ring [24]. This selectivity increase is almost entirely due to a decrease in the $D_2$ affinity, indicating that in contrast to the affinity for the $D_4$ receptor, the $D_2$ affinity is highly dependent on the electronic properties of the aromatic ring corresponding to pharmacophore element **A** (Figure 11). Similarly, the $D_2/D_4$ selectivity increases from 4 in compound **22** to 54 in compound **23** [38]. Even in this case the $D_4$ affinity is largely unaffected.



*Figure 9.* A least-squares superimposition of the proposed bioactive conformations of compounds **5–7** and **16–18**.



21        22        23

Liégeois et al. [39] have shown that replacing the phenyl ring corresponding to pharmacophore element **B** in clozapine (**3**) analogs by a pyridyl ring increases the $D_2/D_4$ selectivity by a factor of 12. Again the $D_4$ affinity is virtually unaffected, whereas the $D_2$ affinity decreases. The dependence of the affinity for $D_2$ receptors on the electronic properties of aromatic rings is also observed in pyrazole analogs of compound **16**. Replacement of the p-chlorophenyl ring by a cyclohexyl ring gives a moderate $D_4$ selectivity ($D_2/D_4 = 6$). Replacing the cyclohexyl ring by a pyridyl ring increases the selectivity to 39 [30] through a decrease in the $D_2$ affinity.

by a fluoro group or a sulphonamido group has only a marginal effect on the $D_4$ affinity. However, at the $D_2$ receptor the affinity decreases by a factor of 27 by replacing the fluoro substituent by a sulphonamido group. This difference indicates that there is more space in the $D_4$ receptor that in the $D_2$ receptor in the environment of the methoxy substituent in **11**. This information is shown in Figure 11 within the framework of the $D_4$ and $D_2$ pharmacophore models as a receptor essential volume **H** in the $D_2$ receptor not present in the $D_4$ receptor. Recently, Beliotti et al. [40] reported $D_2$ and $D_4$ affinities for a series of 6- and 7-piperazinyl- and piperidinylmethylbenzoxazinones. Also in these series of compounds an increase of the substituent size in the position corresponding to the methoxy group position in **11** significantly de-
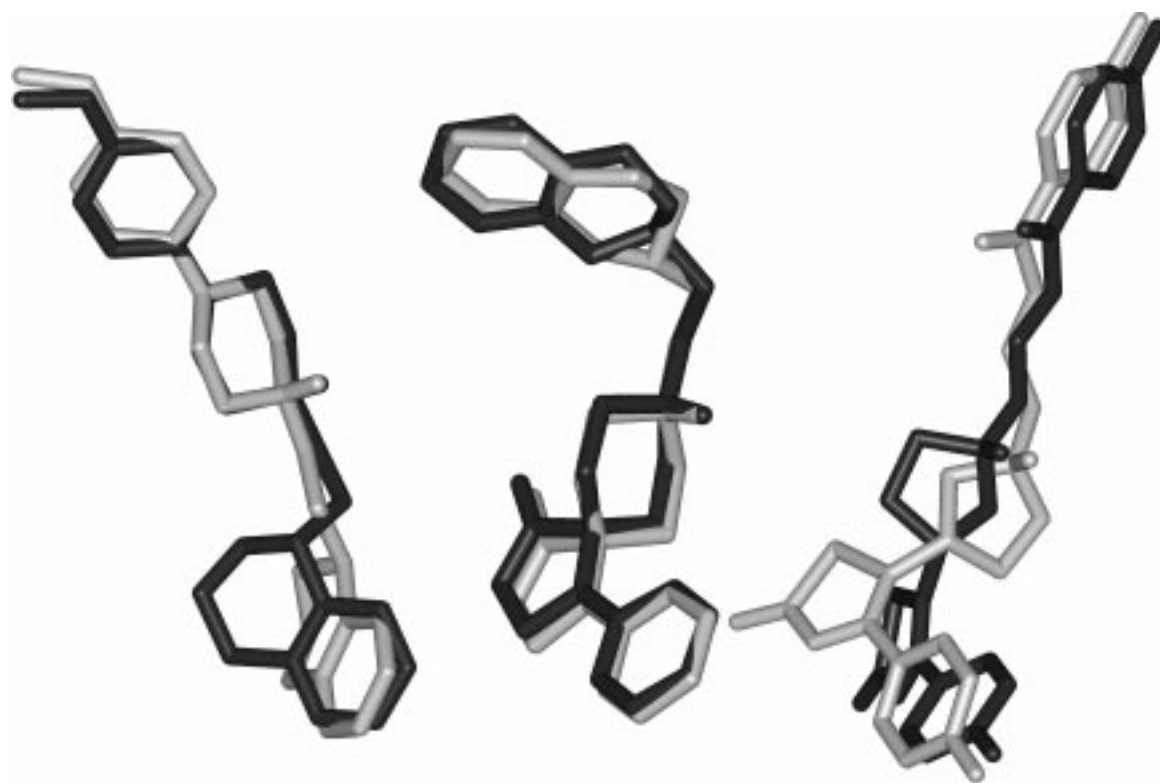
784



*Figure 10.* A least-squares superimposition of the enantiomers of **11**, **12** and **18** as fitted to the pharmacophore model. The (S)-enantiomers are shown in light grey and the (R)-enantiomers in dark grey. Hydrogens are removed for clarity.

A highly selective $D_4$ antagonist generally requires a molecular part corresponding to pharmacophore element **G** (Figure 11). Tricyclics with small N-substituents are generally non-selective as shown by the representative examples in Table 1. This clearly indicates that receptor interactions with the molecular part corresponding to pharmacophore element **G** are highly important for the $D_2/D_4$ selectivity. The nonselective butyrophenones **5**–**7** and the highly selective $D_4$ antagonist **18** all fit well to the $D_4$ and $D_2$ pharmacophore models in low energy conformations (Table 1, Figure 9). It is obvious that the source of selectivity (see Table 1) is to be found in the electronic and/or steric differences in the parts of the molecules corresponding to pharmacophore element **G**. This is also demonstrated by the observation that the indole analog of **15** displays a $D_2/D_4$ selectivity of 44 which increases to 2233 for the azaindole compound **15** [29]. This selectivity increase is the result of a decrease of the $D_2$ affinity and a small increase of the $D_4$ affinity. A similar selectivity increase was observed by Showell et al. for the corresponding replacement in compound

**17** [31]. Also in this case selectivity increase is almost entirely due to a decrease of the $D_2$ affinity.

In summary, changes in the electronic properties of the molecular parts corresponding to pharmacophore elements **A**, **B** and **G** may result in a substantial decrease of the $D_2$ affinity whereas the $D_4$ affinity generally is largely unaffected. This difference must be due to differences in the properties of the corresponding receptor sites with which the pharmacophore elements are interacting. A rationalization of selectivity on this basis is outside the scope of pharmacophore models. However, on the basis of pharmacophore models such differences in interactions may be investigated by, for instance, 3D QSAR methodology. Complementary information may be obtained by studying 7TM receptor models of the corresponding receptors in order to try to identify differences in the amino acid composition in a putative antagonist binding-site. Investigations along these lines are currently in progress.
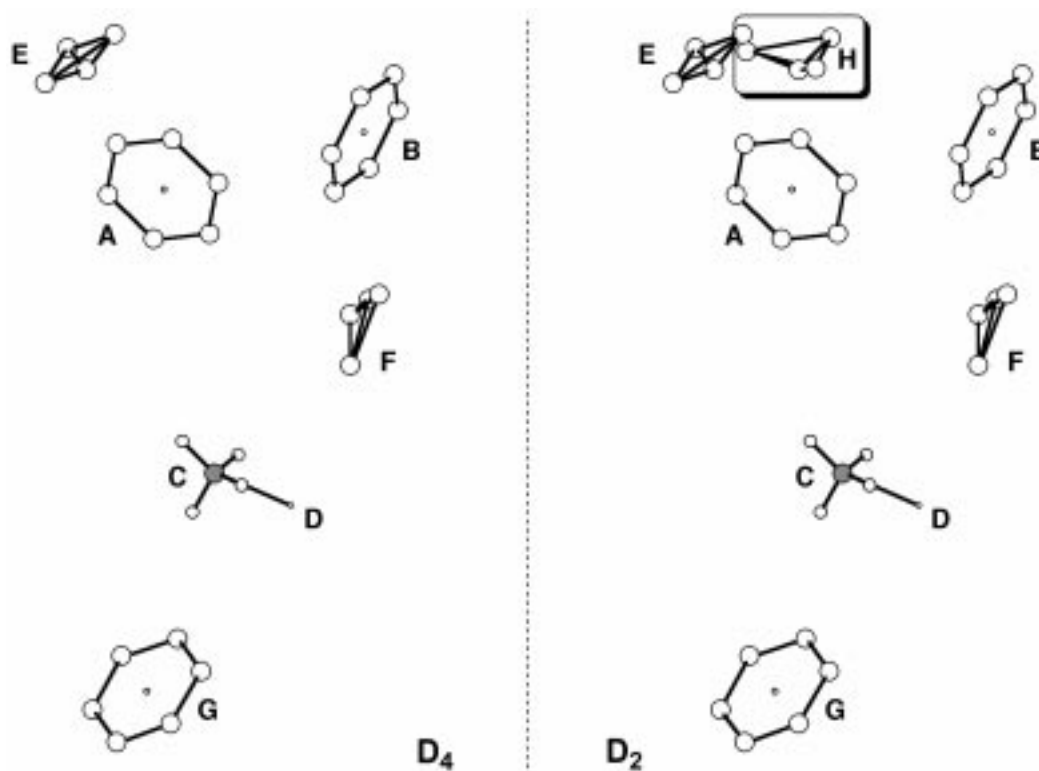
*Figure 11.* The final $D_4$ and $D_2$ pharmacophore models including the receptor essential volume **H** in the $D_2$ model.

## Conclusions

A pharmacophore model for DA $D_4$ antagonists has been developed on the basis of a previously reported DA $D_2$ model. In this connection the $D_2$ model has been further extended. Eighteen structurally diverse antagonists have been fitted to the $D_4$ and $D_2$ models. The model has successfully been used to rationalize enantioselectivities for chiral antagonists. It is concluded that the bioactive conformations of antagonists at the two receptor subtypes are virtually identical. Receptor essential volumes previously identified for the $D_2$ receptor are also present in the $D_4$ receptor. However, a receptor essential volume in the $D_4$ receptor not present in the $D_2$ receptor has been identified. This feature may be exploited for the design of $D_4$ selective antagonists. It is concluded that the major determinant of $D_2$/$D_4$ selectivity is the interactions between the receptor and the pharmacophore elements **A**, **B** and **G** corresponding to aromatic ring systems present in virtually all antagonists. In particular, the effect of the electronic properties of these pharmacophore elements on the affinities for the two receptor subtypes differs substantially, the DA $D_2$ receptor being significantly more dependant than the $D_4$ receptor on the nature of these electronic properties. The pharmacophore models may be employed in 3D QSAR studies in order to obtain a more detailed insight into the relationships between the electronic properties of the aromatic rings and the $D_2$/$D_4$ selectivity.

## Acknowledgements

## References

1. Seeman, P., Synapse, 1 (1987)133.
2. Casey, D.E., Schizophrenia Res., 4 (1991)109.
3. Matsumoto, M., Hidaka, K., Tada, S., Tasaki, Y. and Yamaguchi, T., Mol. Brain Res., 29 (1995) 157.
4. Bruhwyler, J., Chleide, E. and Mercier, M., Neuroleptic. Neurosci. Biobehav. Rev., 14 (1990) 357.
5. Van Tol, H.H.M., Bunzow, J.R., Guan, H.-C., Sunahara, R.K., Seeman, P., Niznik, H.B. and Civelli, O., Nature, 350 (1991) 610.

6. a. Hadley, M.S., Med. Res. Rev., 16 (1996) 507.
   b. Kulagowski, J.J. and Patel, S., Curr. Pharmaceut. Des., 3 (1997) 355.
   c. Steiner, G., Bach, A., Bioalojan, S., Greger, G., Hege, H.-G., Höger, T., Jochims, K., Munschauer, R., Neuman, B., Teschendorf, H.-J., Traut, M., Unger, L. and Gross, G., Drugs Future, 23 (1998) 191.

7. Liljefors, T. and Bøgesø, K.P., J. Med. Chem., 31 (1988) 306.

8. Bøgesø, K.P., Liljefors, T., Arnt, J., Hyttel, J. and Pedersen, H., J. Med. Chem., 34 (1991) 2023.

9. Palm, J., Bøgesø, K.P. and Liljefors, T., J. Med. Chem., 36 (1993) 2878.

10. Pettersson, I. and Liljefors, T., J. Med. Chem., 35 (1992) 2355.

11. Palm, J.A., Ph.D. Thesis, University of Lund, Sweden, 1990.

12. Bøgesø, K.P. and Sommer, M.B., Collect. Czech. Chem. Commun., 56 (1991) 2456.

13. Andersen, K., Liljefors, T., Gundertofte, K., Perregaard, J. and Bøgesø, K.P., J. Med. Chem., 37 (1994) 950.

14. MacroModel V6.5: Mohamadi, F., Richards, N.G.J., Guida, W.C., Liskamp, R., Lipton, M., Caufield, C., Chang, G., Hendrikson, T. and Still, W.C., J. Comput. Chem., 11 (1990) 440.

15. The MM3(94) program is available to all users from the Technical Utilization Corporation, Inc., Powell, OH, or from Tripos Associates, St. Louis, MO, and to academic users from the QCPE, University of Indiana, Bloomington, IN.

16. Chang, G., Guida, W.C. and Still, W.C., J. Am. Chem. Soc., 111 (1989) 4379.

17. Still, W.C., Tempczyk, A., Hawley, R.C. and Hendrickson, T., J. Am. Chem. Soc., 112 (1990) 6127.

18. Boström, J., Norrby, P.-O. and Liljefors, T., J. Comput.-Aided Mol. Design, 12 (1998) 383.

19. MacMimic, InStar Software AB, Ideon Research Park, Lund, Sweden.

20. a. McMartin, C. and Bohacek, R., J. Comput.-Aided Mol. Design, 11 (1997) 333.
    b. McMartin, C. and Bohacek, R., J. Comput.-Aided Mol. Design, 9 (1995) 237.

21. Gaussian 98, Revision A.7, Frisch, M.J., Trucks, G.W., Schlegel, H.B., Scuseria, G.E., Robb, M.A., Cheeseman, J.R., Zakrzewski, V.G., Montgomery, J.A., Jr., Stratmann, R.E., Burant, J.C., Dapprich, S., Millam, J.M., Daniels, A.D., Kudin, K.N., Strain, M.C., Farkas, O., Tomasi, J., Barone, V., Cossi, M., Cammi, R., Mennucci, B. Pomelli, C., Adamo, C., Clifford, S., Ochterski, J., Petersson, G.A., Ayala, P.Y., Cui, Q., Morokuma, K., Malick, D.K., Rabuck, A.D., Raghavachari, K., Foresman, J.B., Cioslowski, J., Ortiz, J.V., Baboul, A.G., Stefanov, B.B., Liu, G., Liashenko, A., Piskorz, P., Komaromi, I., Gomperts, R., Martin, R.L., Fox, D.J., Keith, T., Al-Laham, M.A., Peng, C.Y., Nanayakkara, A., Gonzalez, C., Challacombe, M., Gill, P.M.W., Johnson, B., Chen, W., Wong, M.W., Andres, J.L., Gonzalez, C., Head-Gordon, M., Replogle, E.S. and Pople, J.A., Gaussian, Inc., Pittsburgh, PA, 1998.

22. AMSOL version 6.1, Hawkins, G.H., Giesen, D.J., Lynch, G.C., Chambers, C.C., Rossi, I., Storer, J.W., Rinaldi, D., Liotard, D.A., Cramer, C.J. and Truhlar, D.G., University of Minnesota, Minneapolis, 1997, based in part on AMPAC-version 2.1 by D.A. Liotard, E.F. Healy, J.M. Ruiz and M.J.S. Dewarn, and on the EF routines by F. Jensen.

23. H. Lundbeck A/S, unpublished data.

24. Thurkauf, A., Yuan, J., Chen, X., Shu, X., Wasley, J.W.F., Hutchison, A., Woodruff, K.H., Meade, R., Hoffman, D.C., Donavan, H. and Jones-Hertzog, D.K., J. Med. Chem., 40 (1997) 1.

25. Nakazato, A., Kumagai, T., Nagamine, M., Gotou, M., Chaki, S., Yoshikawa, R., Suzuki, Y., Okuyama, S., Yoshida, M. and Tomisawa, K., poster, 214th National Meeting of the American Chemical Society, Las Vegas, NV, September 7–11, 1997.

26. Wright, J.L., Gregory, T.F., Heffner, T.G., MacKenzie, R.G., Pugsley, T.A., Vander Meulen, S. and Wise, L.D., Bioorg. Med. Chem. Lett., 7 (1997) 1377.

27. TenBrink, R.E., Berg, C.L., Duncan, J.N., Harris, D.W., Huff, R.M., Lahti, R.A., Lawson, C.F., Lutzke, B.S., Martin, I.J., Rees, S.A., Schlachter, S.K., Sih, J.C. and Smith, M.W., J. Med. Chem., 39 (1996) 2435.

28. Peglion, J.-L., Dessinges, A. and Goument, B., EP-745591 (1996).

29. Kulagowski, J.J., Broughton, H.B., Curtis, N.R., Mawer, I.M., Ridgill, M.P., Baker, R., Emms, F., Freedman, S.B., Marwood, R., Patel, S., Ragan, C.I. and Leeson, P.D., J. Med. Chem., 39 (1996) 1941.

30. Rowley, M., Collins, I., Broughton, H.B., Davey, W.B., Baker, R., Emms, F., Marwood, R., Patel, S., Patel, S., Ragan, C.I., Freedman, S.B., Ball, R. and Leeson, P.D., J. Med. Chem., 40 (1997) 2374.

31. Showell, G.A., Emms, F., Marwood, R., O'Connor, D., Patel, S. and Leeson, P.D., Bioorg. Med. Chem. Lett., 6 (1998) 1.

32. Okuyama, S., Nakazato, A., Kumagai, T., Nagamine, M., Gotou, M., Chaki, S., Yoshikawa, R., Suzuki, Y., Yoshida, M. and Tomisawa, K., Poster 214th National Meeting of the American Chemical Society, Las Vegas, NV, September 7–11, 1997.

33. Perregaard, J., Arnt, J., Bøgesø, K.P., Hyttel, J. and Sánchez, C., J. Med. Chem., 35 (1992) 1092.

34. Janssen, P.A.J. and Awouters, F.H.L., Arzneim. Forsch., 44 (1994) 269.

35. Perregaard, J., Bang-Andersen, B., Pedersen, H., Mikkelsen, I. and Dancer, R., WO-98/28293, 1998.

36. Carling, R.W., Moore, K.W., Moyes, C.R., Jones, E.A., Bonner, K., Emms, F., Marwood, R., Patel, S., Patel, S., Fletcher, A.E., Beer, M., Sohal, B., Pike, A. and Leeson, P.D., J. Med. Chem., 42 (1999) 2706.

37. Nikam, S.S., Martin, A.R. and Nelson, D.L., J. Med. Chem., 31 (1988) 1965.

38. Nakazato, A., Kumagai, T., Nagamine, M., Kondoh, K., Chaki, S., Yoshikawa, R., Funakoshi, T., Okuyama, S., Yoshida, M. and Tomisawa, K., Poster, 216th National Meeting of the American Chemical Society, Boston, MA, August 23–27, 1998.

39. a. Liegeois, J.-F., Bruhwyler, J., Damas, J., Rogister, F., Masereel, B., Geczy, J. and Delarge, J., Eur. J. Pharmacol., 273 (1995) R1.
    b. Liegeois, J.-F., Bruhwyler, J., Damas, J., Nguyen, T.P., Chleide, E.M.G., Mercier, M.G.A., Rogister, F.A. and Delarge, J.E., J. Med. Chem., 36 (1993) 2107.

40. Belliotti, T.R., Wustrow, D.J., Brink, W.A., Zoski, K.T., Shih, Y.-H., Whetzel, S.Z., Georgic, L.M., Corbin, A.E., Akunne, H.C., Heffner, T.G., Pugsley, T.A. and Wise, L.D., J. Med. Chem., 42 (1999) 5181.